GLIA

GLIA 59:1754–1769 (2011)

Proteomic Identification of Novel Targets Regulated by the Mammalian Target of Rapamycin Pathway During Oligodendrocyte Differentiation

WILLIAM A. TYLER,[1] MOHIT RAJA JAIN,[2] STACEY E. CIFELLI,[1] QING LI,[2] LI KU,[3] YUE FENG,[3] HONG LI,[2] AND TERESA L. WOOD[1]*

[1]*Department of Neurology and Neuroscience, New Jersey Medical School Cancer Center, University of Medicine and Dentistry of New Jersey, Newark, NJ*

[2]*Center for Advanced Proteomic Research and Department of Biochemistry and Molecular Biology, New Jersey Medical School Cancer Center, University of Medicine and Dentistry of New Jersey, Newark, NJ*

[3]*Department of Pharmacology, School of Medicine, Emory University, Atlanta, GA*

KEY WORDS
mTOR; myelin; iTRAQ; Fyn; quaking

ABSTRACT
Previous work from our laboratory demonstrated that the mammalian target of rapamycin (mTOR) is active during and required for oligodendrocyte progenitor cell (OPC) differentiation. Here, we applied an iTRAQ mass spectrometry-based proteomic approach to identify novel targets of the mTOR pathway during OPC differentiation. Among the 978 proteins identified in this study, 328 (34%) exhibited a greater than 20% change ($P < 0.05$) in control versus rapamycin-treated cultures following 4 days of differentiation *in vitro*. Interestingly, 197 (20%) proteins were elevated in rapamycin-treated cultures, while 131 (13%) proteins were downregulated by rapamycin. In support of our previous data, inhibiting mTOR caused a dramatic reduction in the expression of myelin proteins. mTOR also was required for the induction of proteins involved in cholesterol and fatty acid synthesis, as well as the expression of many cytoskeletal proteins, cell signaling components, and nuclear/transcriptional regulators. Of particular interest was the identification of several critical mediators of oligodendrocyte differentiation. Specifically, mTOR activity controls the developmentally programmed upregulation of the prodifferentiation factors Fyn and Quaking, whereas the expression of the differentiation repressor Gpr17 was elevated by mTOR inhibition. These data reveal a distinct signature of mTOR-regulated protein expression during OPC differentiation.

INTRODUCTION

The generation of oligodendrocytes and the formation of myelin occur via the terminal differentiation of the oligodendrocyte progenitor cell (OPC). As differentiation occurs in response to a combination of intrinsic and extrinsic cues, OPCs withdraw from the cell cycle and undergo a dramatic change in morphology by extending highly branched processes that engage and wrap around axon segments to initiate myelination. The mechanisms that drive OPC differentiation and myelination remain unclear. However, previous work from our laboratory and others has identified the mammalian target of rapamycin (mTOR) as a central component of the signal transduction network that promotes the generation of mature oligodendrocytes and myelin (Goebbels et al., 2010; Harrington et al., 2010; Narayanan et al., 2009; Tyler et al., 2009; Zou et al., 2011).

mTOR is a member of the phosphatidylinositol 3-kinase-like family of serine-threonine kinases that integrates signaling from growth factor stimulation and nutrient sensing to modulate a number of biological processes including cell growth, proliferation, protein translation, differentiation, and autophagy [for review, see Sarbassov et al. (2005)]. mTOR forms two intracellular signaling complexes termed mTORC1 and mTORC2, defined respectively by the association of mTOR with the adaptor proteins raptor or rictor that direct mTOR's kinase activity toward distinct downstream signaling effectors (Kim et al., 2002; Sarbassov et al., 2004). Previously, we demonstrated that both mTORC1 and mTORC2 act through unique mechanisms to direct the timing of oligodendrocyte differentiation (Tyler et al., 2009). Specifically, inhibiting mTORC2 during OPC differentiation caused a reduction in the mRNA levels of several key myelin genes, whereas inhibiting mTORC1 resulted in decreased myelin protein levels most likely by interfering with the translation of these transcripts. However, the targets of the mTOR pathway that regulate oligodendrocyte differentiation are unknown.

To identify global changes in the proteome during OPC differentiation *in vitro* and novel targets of the mTOR pathway, we performed iTRAQ-proteomics analysis of proteins isolated from cultures of OPCs differenti-

Additional Supporting Information may be found in the online version of this article.

William A. Tyler, Mohit Raja Jain, and Stacey E. Cifelli contributed equally to this work.

Grant sponsor: National Institutes of Health; Grant numbers: NS37560, NS056097 and 5P30NS046593; Grant sponsor: National Multiple Sclerosis Society; Grant number: RG4015A2/2.

*Correspondence to: Teresa L. Wood, Department Neurology and Neuroscience, University Hospital Cancer Center H1200, New Jersey Medical School/UMDNJ, 205 S. Orange Ave, Newark, NJ 07101-1709. E-mail: woodte@umdnj.edu

Received 13 January 2011; Accepted 22 June 2011

DOI 10.1002/glia.21221

Published online 19 August 2011 in Wiley Online Library (wileyonlinelibrary.com).

ated in the presence or absence of rapamycin, a specific inhibitor of mTOR kinase activity. The iTRAQ-based technology uses a series of molecular weight tags that covalently label the N-termini and Lys side chain amines of peptides, which serve as a sample-specific reporter and enable the multiplexed relative quantification of protein levels. Using this approach, we have identified a unique mTOR-dependent protein expression signature during OPC differentiation.

MATERIALS AND METHODS

Reagents

Cell-culture media (MEM, DMEM/F12), FBS, trypsin, and insulin-selenium-transferrin were purchased from GIBCO-BRL (Long Island, NY). Additional N2 supplements, triiodothyronine, and poly-D-lysine were purchased from Sigma (St. Louis, MO). Recombinant human FGF-2 was purchased from R&D Systems (Minneapolis, MN). Rapamycin was purchased from Calbiochem (San Diego, CA). The anti-βIV tubulin antibody was purchased from Sigma. The antisirtuin-2 antibody was purchased from Cell Signaling (Danvers, MA). Triethylammonium bicarbonate buffer (TEAB), IGEPAL® CA-630, Triton® X-100, Protease Inhibitor Cocktail, phosphatase inhibitor cocktail I, and phosphatase inhibitor cocktail II were from Sigma. Tris(2-carboxyethyl)-phosphine (TCEP), methyl methanethiosulfonate (MMTS), iTRAQ reagents were from Applied Biosystems (ABI, Foster City, CA). Sequencing grade-modified trypsin was from Promega Corp. (Madison, WI). PepClean™ C18 spin columns were from Pierce (Rockford, IL).

Primary Cortical Oligodendrocyte Progenitor Cultures and Differentiation Paradigm

OPCs were purified from cortical mixed glial cultures prepared from postnatal days 0–2 Sprague–Dawley rat pups as previously described (McCarthy and de Vellis, 1980; Tyler et al., 2009). Purified OPCs were seeded onto poly-D-lysine-coated T75 flasks at a density of 2×10^4 cells/cm^2 in a chemically defined medium (N2S) consisting of 66% N2B2 (DMEM/F12 supplemented with 0.66 mg/mL BSA, 10 ng/mL D-biotin, 5 μg/mL insulin, 20 nM progesterone, 100 μM putrescine, 5 ng/mL selenium, 50 μg/mL apo-transferrin, 100 U/mL penicillin, 100 μg/mL streptomycin, and 0.5% FBS) supplemented with 34% B104 conditioned media, 5 ng/mL FGF, and 0.5% FBS. Purified OPCs were amplified for 4–10 days in N2S, passaged once with papain, and plated for experiments. OPC differentiation was initiated using an established mitogen withdrawal protocol in the presence of 30 ng/mL triiodothyronine (T3) in the presence or absence of 10 nM rapamycin as described previously (Tyler et al., 2009). Control cultures received vehicle alone (0.002% ethanol). N2B2 + T3 differentiation media with or without rapamycin was replenished every 48 h during the course of experiments.

Protein Extraction and iTRAQ Labeling

OPCs differentiated in the presence or absence of rapamycin (10 nM) were rinsed with PBS, pelleted by centrifugation at 10,000*g* for 8 min, and stored at −80°C before use. The cell pellets were briefly thawed on ice and resuspended in a lysis buffer consisting of 500 mM TEAB, 1.0% Igepal CA630, 1.0% Triton X-100, protease inhibitor cocktail (Sigma), phosphatase inhibitor cocktail I (Sigma), and phosphatase inhibitor cocktail II (Sigma). The supernatant was cleared by centrifugation at 16,100*g* for 30 min at 4°C, and the pH was adjusted to 8.0 with 1.0 M TEAB. One hundred micrograms of proteins from each sample were used for this analysis. After reduction with TCEP and alkylation with MMTS, tryptic digestion was performed by addition of 5 μg of trypsin (Promega Corporation) to each of the eight samples at 37°C for overnight. Peptides derived from the four different control OPC cultures were labeled with iTRAQ tags 113, 114, 115, and 116, whereas peptides obtained from the four different rapamycin-treated OPC cultures were labeled with tags 117, 118, 119, and 121 as per manufacturer's instructions. The labeled samples were then mixed together and fractionated via two-dimensional liquid chromatography according to procedures described earlier (Jain et al., 2009). The HPLC eluent was mixed with matrix solution (7 mg/mL α-cyano-4-hydroxycinnamic acid, in 50% acetonitrile, 5 mM of ammonium monobasic phosphate) and the internal mass calibrants (50 fmol/μL each of [Glu1]-fibrinopeptide B and adrenocorticotropic hormone fragment 18–39) through a 30-nL mixing tee before directly spotting onto 1,650 well MALDI plates. For a follow-up time course study, samples were processed similarly except peptides were labeled as follows: 2-day control OPC with iTRAQ tags 113 and 114, 2-day rapamycin-treated OPC with iTRAQ tags 115 and 116, 4-day control OPC with iTRAQ tags 117 and 118, and 4-day rapamycin-treated OPC with iTRAQ tags 119 and 121.

MALDI–TOF/TOF Tandem MS Analysis

The peptides were analyzed on an ABI 4800 Plus MALDI TOF/TOF™ Analyzer with 4000 series explorer software (version 3.5.3) in a data-dependent fashion, using a job-wide interpretation method (Jain et al., 2008). MS spectra (m/z 800–3,600) were acquired in positive ion refelectron mode with internal mass calibration. Total of 1,000 laser shots were accumulated for each spot. A maximum of fifteen most intense ions ($S/N \geq 50$) per spot were selected for succeeding MS/MS analysis in 2.0 keV mode, using air as a CID gas at a pressure of 5×10^{-7} Torr. A total of 4,000 laser shots were accumulated for each spectrum.

Protein Database Search and Bioinformatics

TS2Mascot (Matrix Science, London, UK) was used to generate the peak lists as mascot generic file from tandem mass spectra, using following parameters (mass

range form 20–60 Da below precursor, S/N ratio $\geq$ 10). All MS/MS data were analyzed using Mascot (Matrix Science, London, UK; version 2.3.02) and X! Tandem (The GPM, thegpm.org; version 2007.01.01.1). Mascot and X! Tandem was set up to search the concatenated International Protein Index (IPI) rat database (version 3.74, containing 39708 forward and 39708 reverse entries) assuming trypsin as the digestion enzyme. Mascot and X! Tandem were searched with a fragment ion mass tolerance of 0.30 Da and a parent ion tolerance of 50 parts per million. MMTS of cysteine, +304 (iTRAQ) of lysine, and +304 (iTRAQ) of the N-termini were specified in Mascot and X! Tandem as fixed modifications. Oxidation of methionine and iTRAQ 8plex modification of tyrosine were specified as variable modifications. Scaffold (version 3.00.03, Proteome Software, Portland, OR) was used to validate MS/MS-based peptide and protein identifications. Peptide identifications were accepted if they could be established at greater than 95.0% probability as specified by the Peptide Prophet algorithm (Keller et al., 2002). Protein identifications were accepted if they could be established at greater than 50.0% probability and contained at least one unique identified peptide. These criteria were chosen so that the protein false discovery rate (FDR) remained less than 1%. Protein probabilities were assigned by the Protein Prophet algorithm (Nesvizhskii et al., 2003). Proteins that contained similar peptides and could not be differentiated based on MS/MS analysis alone were grouped together to satisfy the principles of parsimony. Scaffold Q+ (version 3.00.03, Proteome Software, Portland, OR) was used to quantify peptides and proteins. Peptides were quantified using the centroided reporter ion peak intensities. Intrasample channels were normalized based on the median ratio for each iTRAQ channel across all proteins. Protein quantitative values were derived from only uniquely assigned peptide ratios. Scaffold Q+ provided the quantitative ratios as Log2 normalized, which were exported to Excel for conversion into the normal ratios. Protein fold changes were expressed as follows: (average of rapamycin treated)/(average of control). P-values were derived from the two-tailed Student's t-test for each protein by comparing the four rapamycin-treated OPCs with the four control OPCs values. Proteins exhibiting a greater than 20% change ($P < 0.05$) were considered significant. The protein population mean ratio was calculated as 1 with a standard deviation of 0.2.

Functional classification of changed proteins was performed by Protein ANalysis THrough Evolutionary Relationships (PANTHER) tool (http://david.abcc.ncifcrf.gov/home.jsp). Proteins not annotated by PANTHER were further annotated at AmiGo (http://geneontology.org). Analysis of possible pathway networks was performed with Ingenuity Pathways Analysis 8.6 (http://www.ingenuity.com).

Comparison with Microarray Data Set

We compared the dynamics of the proteome identified in our study to a published functional genomics analysis of oligodendrocyte differentiation from the same cell type and obtained with a similar experimental procedure for differentiation (Dugas et al., 2006). To compare to our proteomics data, we used the microarray data set from OPCs and 3-day differentiation data points as these conditions paralleled our study. The IPI identifier of the proteomics data were mapped to the microarray probes with common UniGene identifiers. Some of the IPIs mapped to more than one UniGene identifiers in microarray data, and we compared the ratio from the most strongly regulated probeset to the corresponding proteome data. In total, we were able to compare the expression level of 711 proteins with corresponding microarray data. This subset of the proteome was further categorized as explained in the results section.

Western Immunoblotting and Statistical Analyses

Protein isolation and Western immunoblotting were performed as described previously (Tyler et al., 2009). Protein expression levels were quantified using NIH image 1.62. Statistical analyses were performed using StatView statistical analysis software. One-way analysis of variance was performed to test overall significance. Fisher's LSD *post hoc* test was used to determine significance of all pairwise comparisons.

RESULTS

Analysis of mTOR-Dependent Protein Expression During Oligodendrocyte Differentiation

Our previous study demonstrated that mTOR signaling is required for the transition from the $O4^+/GalC^-$ late progenitor to the $O4^+/GalC^+$ immature oligodendrocyte stage *in vitro* (Tyler et al., 2009). Thus, to determine changes in protein expression that corresponded to the mTOR-regulated transition from OPC to mature oligodendrocyte, we performed iTRAQ-MS analysis on quadruplicate protein samples from control and rapamycin (10 nM), a specific inhibitor of mTOR kinase activity, treated cultures on day 4 of differentiation (see Fig. 1).

Overall, we identified 978 unique proteins (Table 1; Supp. Info. Table 1). For each identified peptide, a CI value greater than or equal to 95% was required. Each protein was assigned with at least one unique peptide at less than 1.0% FDR of proteins. A total of 328 (34%) proteins exhibited a greater than 20% change ($P < 0.05$) in control versus Rapamycin-treated cultures. Interestingly, 197 proteins (20%) were elevated in rapamycin-treated OPCs, while 131 proteins (13%) were expressed at a higher level in control cells (Table 1; Supp. Info. Table 1).

Quantification Consistencies Among the Peptides and iTRAQ Experimental Repeats

Our previous studies demonstrated that iTRAQ quantification accuracy is heavily dependent upon ion signal

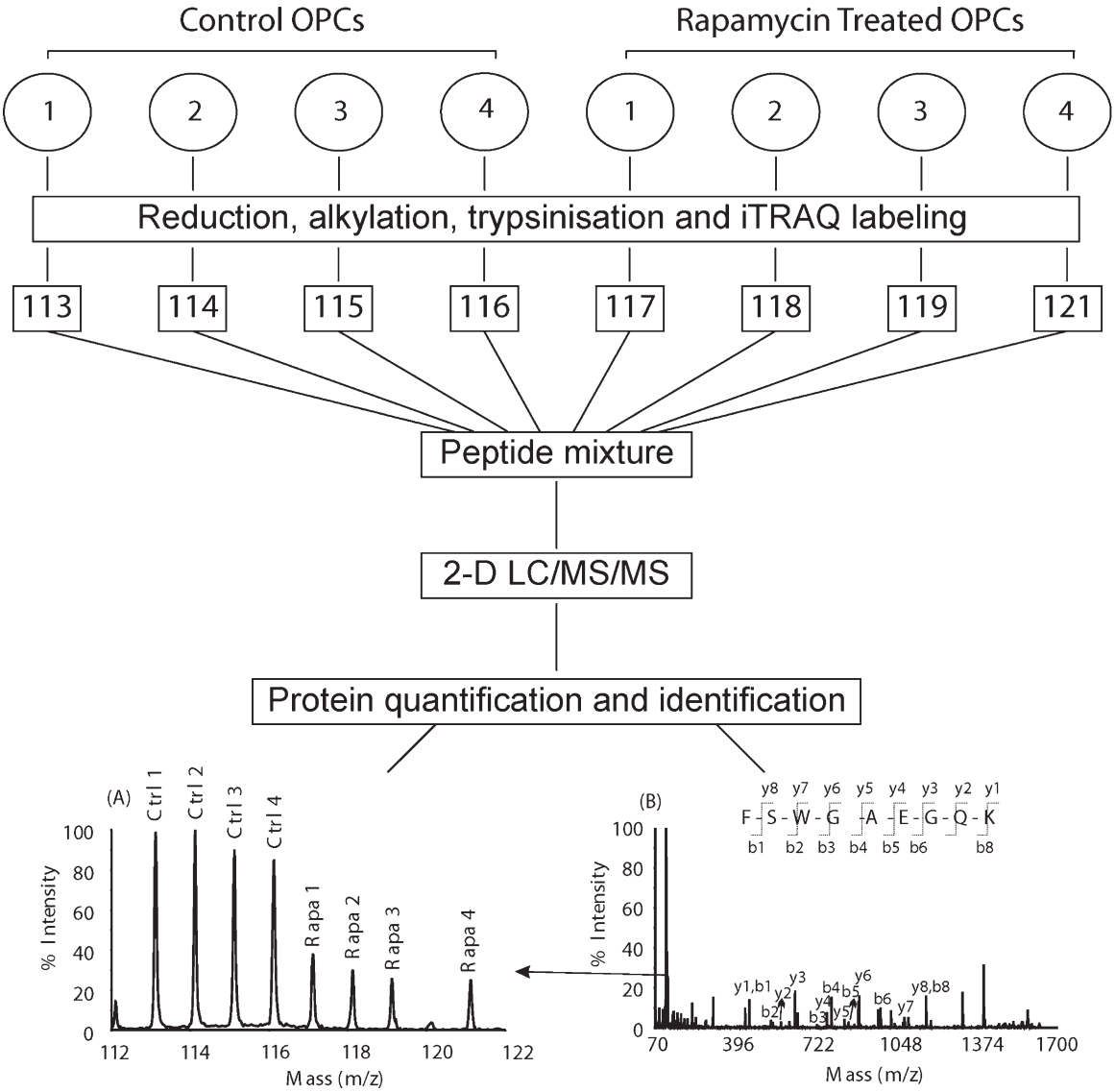

Fig. 1. iTRAQ work flow for the identification of novel targets regulated by the mammalian target of rapamycin pathway during oligodendrocyte differentiation. Proteins from four independent control and rapamycin-treated cells were processed sequentially with disulfide reduction, alkylation, and trypsin digestion. The resulting peptides were individually labeled with the iTRAQ reagents 113–121 as indicated. After quenching of the remaining free iTRAQ reagents, the labeled peptides were mixed together and analyzed by LC/MS/MS for peptide sequencing and quantification.

TABLE 1. Summary of Proteins Identified by iTRAQ-MS Analysis Following 4 Days of Differentiation ±10 nM rapamycin

Unique proteins identified (95% CI)	978
Proteins changed (Ctrl vs. Rapa)	328 (34%)
Proteins decreased (Rapa vs. Ctrl)	131 (13%)
Proteins elevated (Rapa vs. Ctrl)	197 (20%)

intensities and the timed-ion-selector (TIS) window and other factors (Hu et al., 2006). With the ABI 4800 MALDI–TOF–TOF mass spectrometer, we were able to perform the experiment at a TIS window at a maximal resolution of 400 (±2.5 Da at m/z 1,000), which significantly enhanced our peptide quantification consistency over the 4700 model of the instrument. For example, with the aid of the Scaffold Q+ 3.0 software, we were able to demonstrate that a rapamycin versus control (R/C) iTRAQ ion plot (117 vs. 113) of various iTRAQ reporter ion intensities derived from the spectra matched to different tryptic peptides of brain acid soluble protein 1 (BASP-1), revealing similar upregulated 117/113 ratios of ~1.8 (Fig. 2A). Consistent changes for different peptides can also be observed for the downregulated myelin proteolipid protein (PLP) (Fig. 2E). These observations suggest that the 8-plex iTRAQ approach is reliable at determining protein expression change trends, even with a limited number of peptides assigned to a given protein. For a given peptide, the utilization of the 8-plex iTRAQ reagents greatly enhanced our ability to perform a relatively large number of biological repeats to determine significant protein changes (Fig. 2B,C,F,G). At the

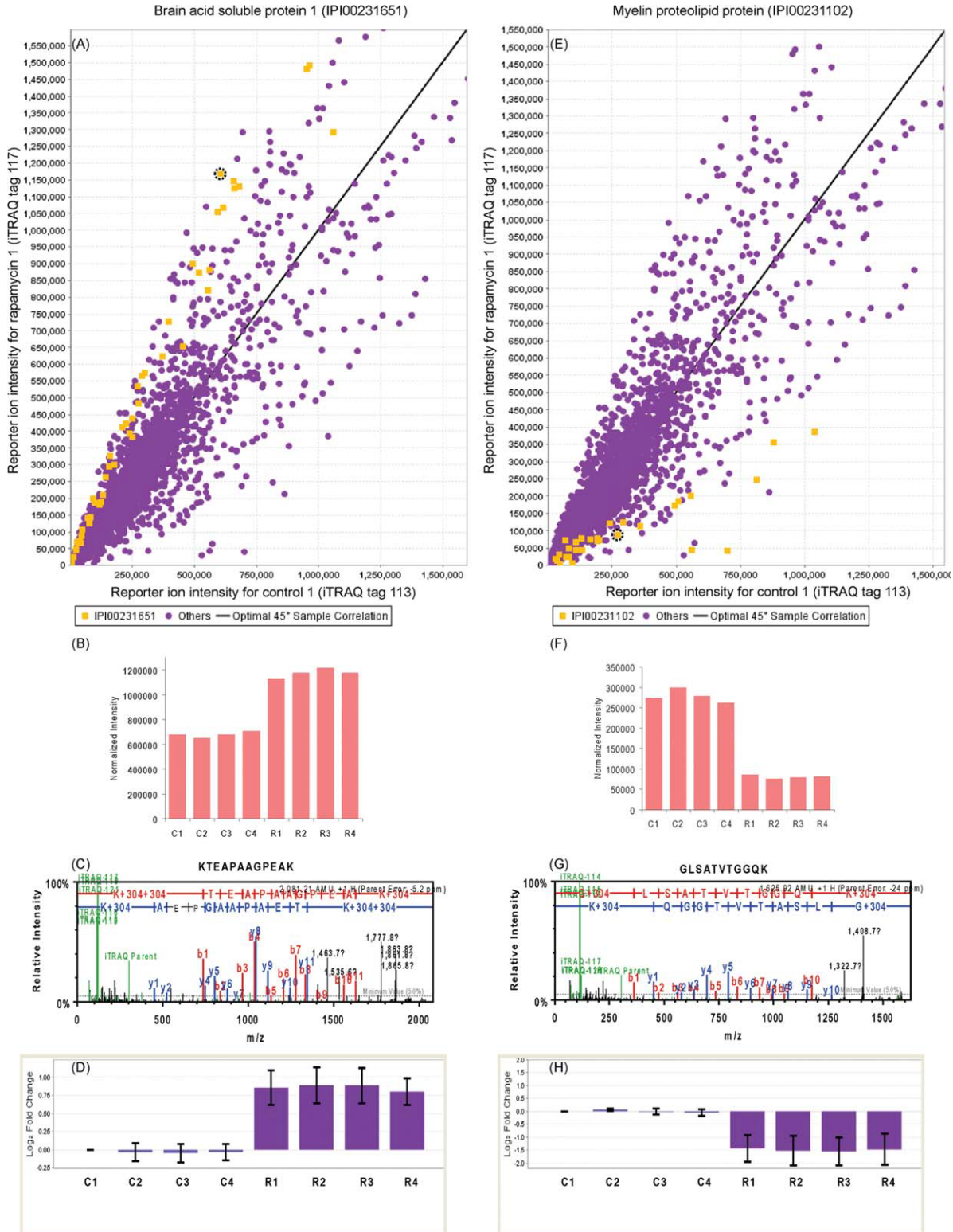

Fig. 2. Upregulation of BASP-1 and downregulation of PLP were ascertained from the consistent iTRAQ ratios obtained from all related precursor ions. **A, E:** Plots of reporter ion 113 (see Fig. 1, Control treatment 1) versus 117 intensities (see Fig. 1, Rapamycin treatment 1) for all identified peptides (purple dots). The iTRAQ plot dots fall near the straight lines represent the peptides that were not differentially regulated by rapamycin treatment. Each yellow dot represents the iTRAQ signals derived from a spectrum matched to a BASP-1 (A) or PLP (E). Peptide plot pairs of various reporter ion intensities matched to BASP-1 revealed similar upregulated 117/113 ratios of ~1.8 and when matched to PLP, 117/113 ratios of ~0.4. **B,F:** Bar graphs of the normalized intensities of the iTRAQ reporter ions for a representative peptide ion (as circled in A and E) of BASP-1 (B) and PLP (F). C1–C4 (control samples), and R1–R4 (rapamycin-treated samples) (see Fig. 1), indicates consistent upregulation of BASP-1 peptide (R/C of ~1.8) and downregulation of PLP peptide (R/C of ~0.3) across all the replica of the experiment. **C,G:** Continuous series of the b and y ions enabled the identification of the peptides as KTEAPAAGPEAK (C, circled in A) and GLSATVTGGQK (G, circled in E). **D,H:** Bar graphs of the means and standard deviations of the protein level iTRAQ ratios in relation to iTRAQ 113 signals obtained from all the peptides derived from either BASP-1 (D) or PLP (H). Error bars indicate quantification variability among the peptides. The means for each independent experiment were very consistent among the replicates (figures were generated using scaffold.)

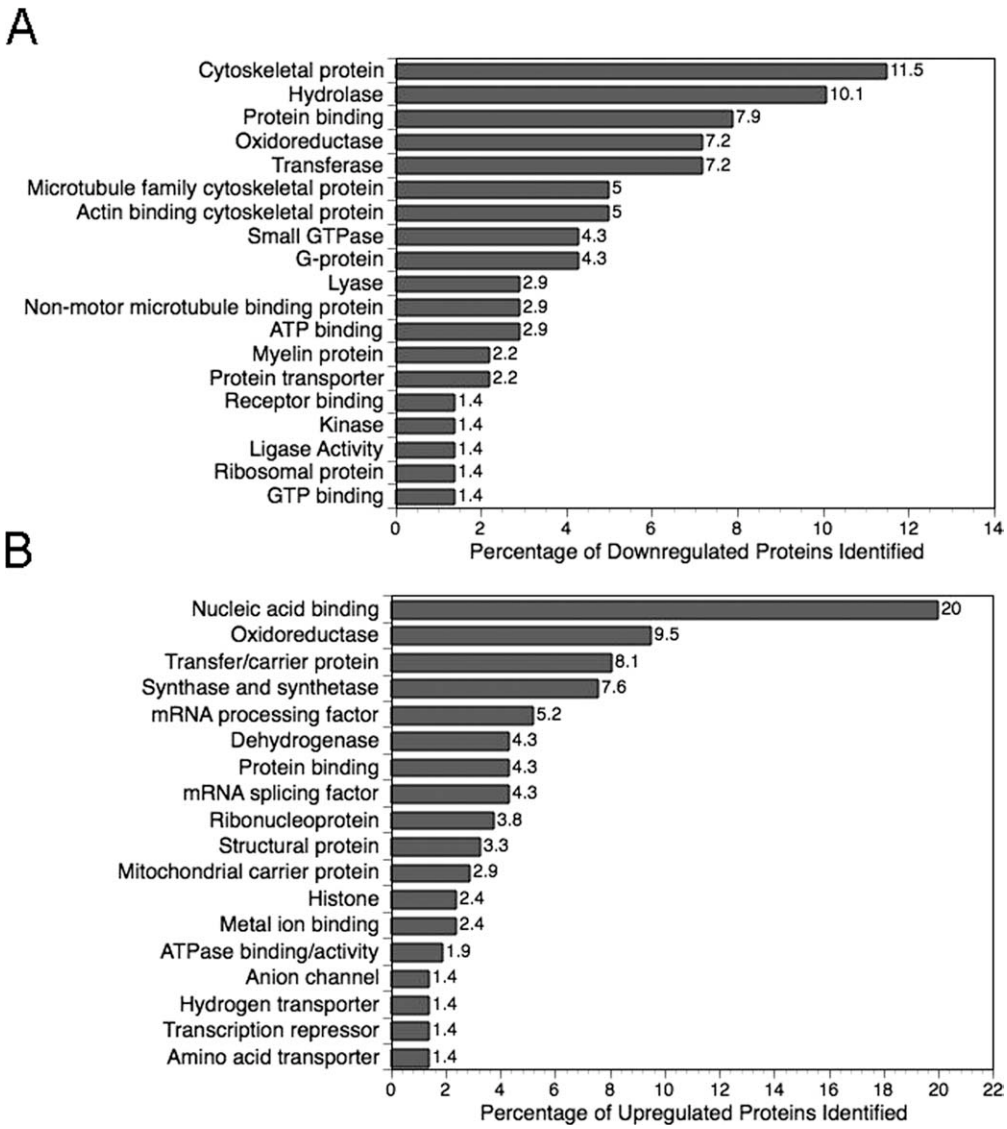

Fig. 3. Functional classification of changed proteins at 4d of OPC differentiation. **A,B:** Functional classification of the top classes of proteins downregulated (A) or upregulated (B) by rapamycin treatment during OPC differentiation.

protein level, the quantification variations among the peptide levels did not significantly affect the mean expression changes of a protein for each iTRAQ-labeled biological repeat (Fig. 2D,H), enabling the determination of significant protein expression changes with the 8-plex iTRAQ approach.

Classification of mTOR-Regulated Proteins

To better characterize mTOR-dependent changes in protein expression during OPC differentiation, we performed analyses using the PANTHER (*P*rotein *AN*alysis *TH*rough *E*volutionary *R*elationships) classification system (Thomas et al., 2003), the AmiGO search database from the Gene Ontology Consortium, and Ingenuity Pathway Analysis. The results of PANTHER analyses by molecular function highlighted major categories of proteins that were negatively regulated by rapamycin treatment and thus normally induced by mTOR (Fig. 3A). Approximately 25% of these proteins were found in cytoskeletal protein subcategories such as cytoskeletal protein (12%), microtubule family cytoskeleton protein (5%), actin-binding cytoskeletal protein (5%), and non-motor microtubule-binding protein (3%) (Fig. 3A). Other categories identified as mTOR-induced included hydrolase (10%), transferase (7%), oxidoreductase (7%), small GTPase (4%), G-protein (4%), and myelin proteins (2%) (Fig. 3A). Similarly, Ingenuity Pathway Analysis revealed a number of proteins downregulated by rapamycin treatment including proteins involved in cholesterol biosynthesis (Idi1, Fdft1, Fdps, and Hmgcs1) and

TABLE 2. Proteins with Known Function in Myelin Synthesis and Oligodendrocyte Differentiation Identified by iTRAQ-MS Analysis Following 4 Days of Differentiation ±10 nM Rapamycin

Gene symbol	Name	R/C (4 days)	Unique peptide count (>95% CI)
Cholesterol BioSynthesis			
Idi1	Isopentenyl-diphosphate δ-isomerase	0.7	3
Fdft1	Fdft1 squalene synthase	0.7	3
Fdps	Farnesyl pyrophosphate synthetase	0.7	4
Hmgcs1	Hydroxymethylglutaryl-CoA synthase	0.6	2
Fatty acid biosynthesis			
Acsl3	Isoform short of long-chain-fatty-acid-CoA ligase 3	0.7	3
Acsl4	Long-chain-fatty-acid-CoA ligase 4	0.8	2
Fasn	Fatty acid synthase	0.8	25
Myelin proteins			
PLP	Plp1 myelin proteolipid protein	0.4	7
MAG	Isoform L-MAG of myelin-associated glycoprotein	0.5	4
CNP	2′,3′-cyclic-nucleotide 3′-phosphodiesterase	0.6	28
Ugt-8	2-hydroxyacylsphingosine 1-β-galactosyltransferase	0.6	3
MBP	Isoform 1 of myelin basic protein S	0.7	5
Regulators of differentiation			
Qk	QKI proteinglycoprotein	0.8	2
Fyn	Proto-oncogene tyrosine-protein kinase Fyn	0.8	3
Gpr17	Uracil nucleotide/cysteinyl leukotriene receptor	1.3	2

fatty acid biosynthesis (Acsl3, Acsl4, and Fasn) (Table 2), suggesting that mTOR induces expression of multiple proteins necessary for myelin lipid synthesis. In contrast, functional classification of proteins upregulated in rapamycin-treated cells and thus normally downregulated by mTOR signaling during differentiation included: nucleic acid binding (20%), oxidoreductase (10%), synthase and synthetase (18%), transfer/carrier protein (18%), mRNA processing factor (5%), dehydrogenase (4%), mitochondrial carrier protein (3%), and anion channel (2%) (Fig. 3B).

Consistent with our previously published data, we identified myelin proteins that were downregulated by rapamycin including myelin basic protein (MBP), PLP, myelin-associated glycoprotein, 2′,3′ cyclic nucleotide 3′-phosphodiesterase (CNP), and 2-hydroxyacylsphingosine 1-β-galactosyltransferase (Ugt8) (Table 2 and Fig. 2). Spectral analysis revealed a 40% reduction of MBP in rapamycin-treated cultures (Fig. 4A). Immunostaining for MBP on OPCs differentiated for 5 days confirmed a significant number of MBP^+ oligodendrocytes in control cultures; however, inhibiting mTOR prevented the expression of MBP (Fig. 4B). The proteomic analysis also confirmed alterations in PLP, CNPase, and Ugt8 as downstream of mTOR signaling shown in our previous study (Tyler et al., 2009).

Cytoskeletal mTOR Targets in Differentiating OPCs

Downregulation of myelin proteins as well as cholesterol and lipid synthesis enzymes by mTOR inhibition is consistent with a block in the terminal differentiation of oligodendrocytes. However, we were interested in identifying upstream proteins and processes regulated by mTOR that are involved in the decision to commit to terminal differentiation and in the morphological changes associated with oligodendrocyte differentiation.

Decreased expression of cytoskeletal proteins and factors known to regulate changes in the cytoskeleton resulting from mTOR inhibition was a major feature that emerged from our PANTHER analyses. Two proteins identified in this category were sirtuin 2 (Sirt2), a NAD-dependent deacetylase (North et al., 2003), and βIV-tubulin (Fig. 5A,B; Supp. Info. Table 1). Previous studies have shown that Sirt2 expression increases during OPC differentiation, peaks in mature oligodendrocytes, and is undetectable in astrocytes, microglia or neurons (Li et al., 2007; Werner et al., 2007). Sirt2 deacetylates α-tubulin and modulates microtubule stability in oligodendrocytes (Li et al., 2007; North et al., 2003). βIV-tubulin is an isoform previously identified as a novel oligodendrocyte marker protein that is enriched in premyelinating and actively myelinating oligodendrocytes but undetectable in early OPCs or astrocytes (Terada et al., 2005). Of particular interest from these studies is that the onset and localization of expression for both Sirt2 and βIV-tubulin in the corpus callosum correlates with the *in vivo* time course of p-mTOR shown in our prior studies (Tyler et al., 2009).

Analyses of protein expression validated our proteomic data demonstrating a 10-fold or 4-fold increase in both Sirt2 and βIV-tubulin expression, respectively, by 4d of differentiation; these increased were inhibited by rapamycin (Fig. 5C,D). Similarly, immunostaining for Sirt2 and βIV-tubulin after 3d of differentiation revealed a number of cells with high levels of each protein in the cytoplasm that extended into processes of the differentiating oligodendrocytes in control cultures with far fewer cells detected in cultures treated with rapamycin (Fig. 6).

In contrast to Sirt2 and βIV-tubulin, additional cytoskeletal-related proteins including neuromodulin (Gap-43) and BASP-1 exhibited an elevated level of expression in response to rapamycin treatment in the proteomic analysis (Supp. Info. Table 1; Fig. 2A–D). Gap-43 is pres-

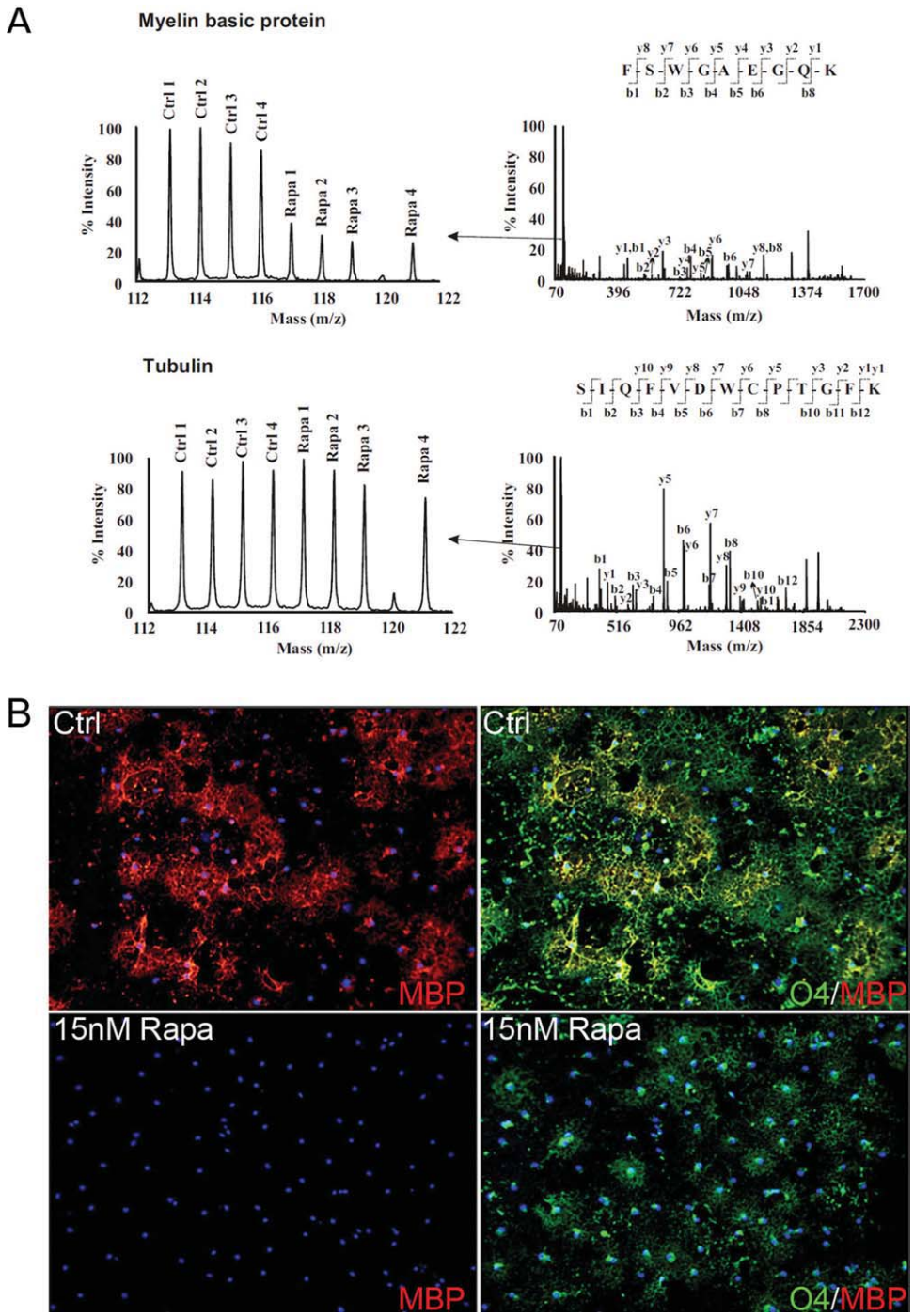

Fig. 4. mTOR activity regulates the expression of myelin basic protein (MBP). **A:** MS/MS spectra for selected peptides. Myelin basic protein was upregulated in Control (4 day) samples and inhibited by rapamycin. Alpha-tubulin was unchanged. Peptide sequences were deduced from the MS/MS spectra based on the observation of continuous series of either N-terminal (b series) or C-terminal (y series) ions. The peak areas of iTRAQ quantification ions, m/z 113–121 were used to measure the relative abundance of individual peptides. **B:** Representative images of MBP (TRITC) and O4 (FITC) IHC are shown for OPCs differentiated for 5 days ± 15 nM rapamycin.

ent in the distal tips of postmigratory oligodendrocytes and plays a role in process extension (Fox et al., 2006). Western blot analyses confirmed that Gap-43 expression decreased by 3d–4d of differentiation in control OPC cultures but remained elevated in rapamycin-treated cultures (Fig. 7A). Similarly, BASP-1, known to regulate neurite outgrowth and actin cytoskeleton (Korshunova et al., 2008; Mosevitsky, 2005), was significantly increased in oligodendrocytes at 4d of differentiation after inhibiting mTOR (Fig. 7B).

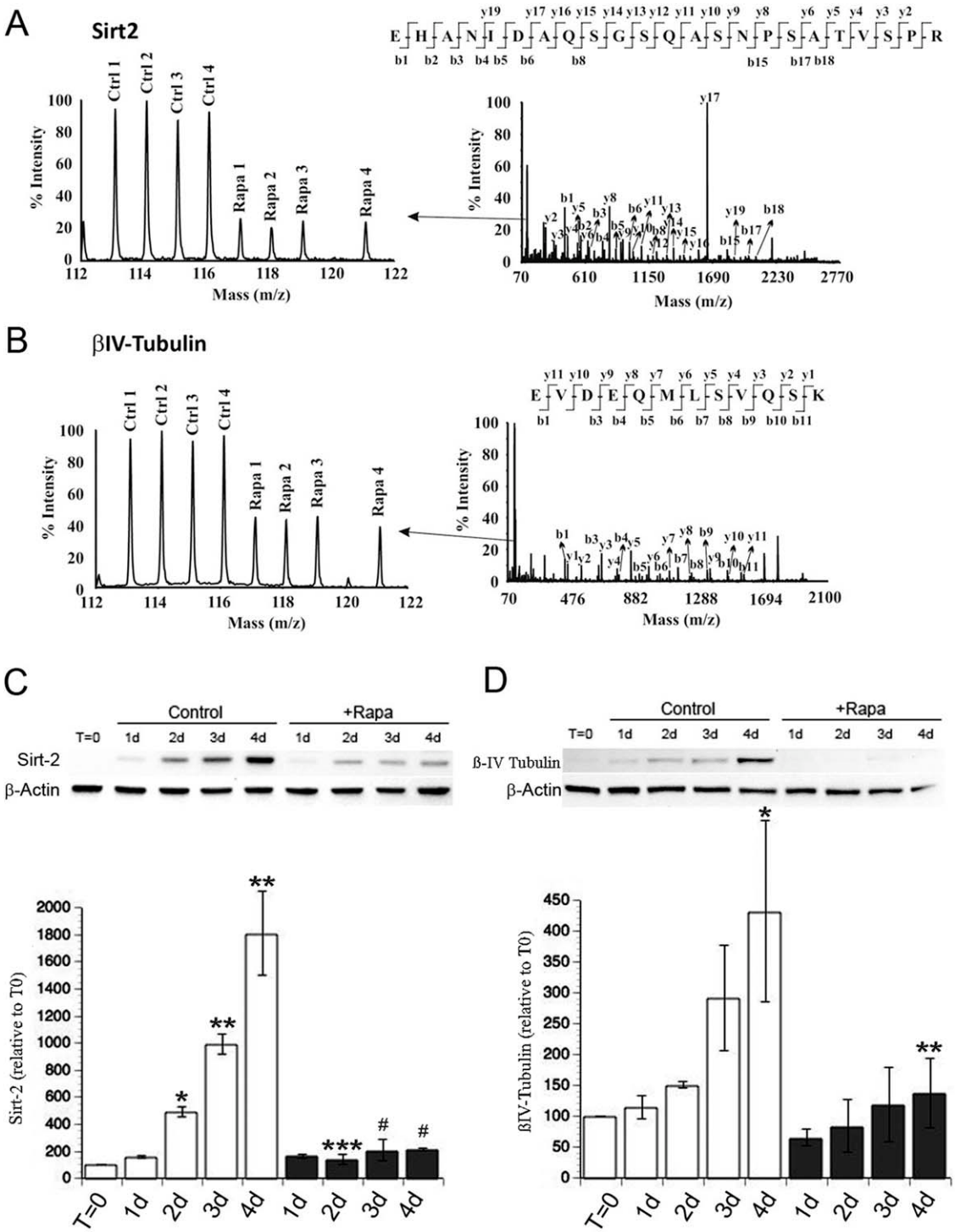

Fig. 5. Identification of Sirt2 and βIV-tubulin as novel targets of the mTOR pathway induced during OPC differentiation. **A, B:** Sirt2 and βIV-tubulin were upregulated in control (4 day) samples and inhbited by rapamycin. Peptide sequences were deduced from the MS/MS spectra based on the observation of continuous series of either N-terminal (b series) or C-terminal (y series) ions. The peak areas of iTRAQ quantification ions, m/z 113–121 were used to measure the relative abundance of individual peptides. **C, D:** Western immunoblot analysis and quantification of Sirt2 (C) and β-IV tubulin (D) expression during a differentiation time course *in vitro*. Results confirm reduced Sirt2 and β-IV tubulin levels with mTOR inhibition. C: $^{*}P = 0.04$ versus 1d ctl; $^{**}P < 0.0001$ versus 1d ctl; $^{***}P = 0.04$ versus 2d ctl, $^{\#}P < 0.0001$ versus 3d and 4d ctl; D: $^{*}P = 0.003$ versus 1d ctl; $^{**}P = 0.004$ versus 4d ctl.

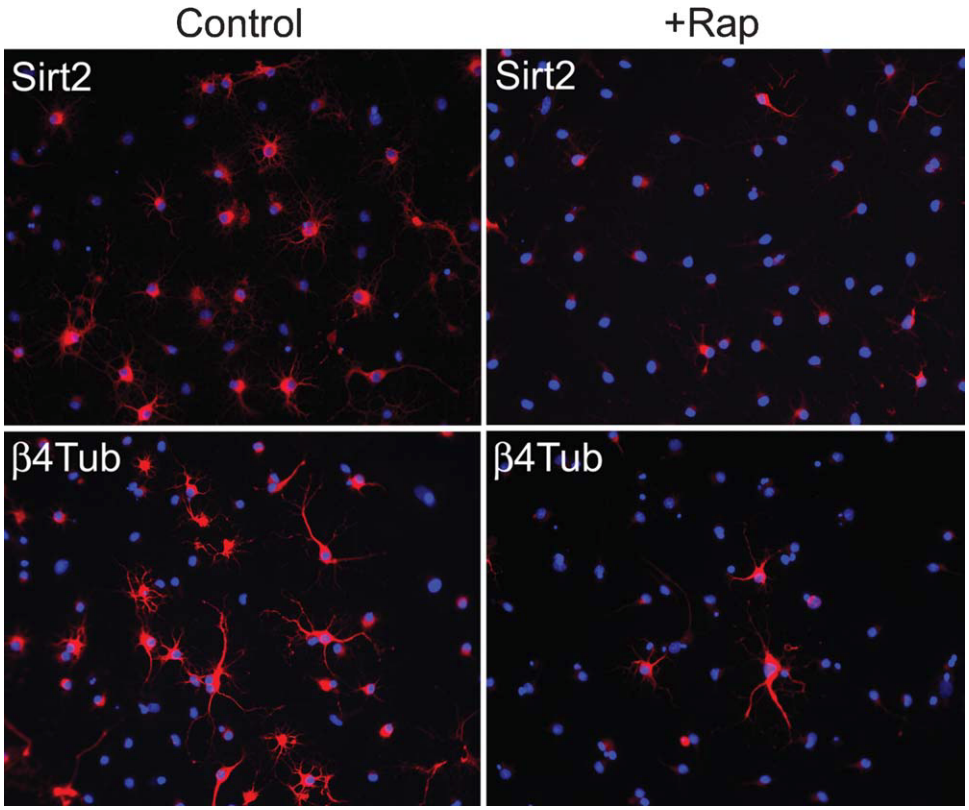

Fig. 6. Sirt2 and βIV-tubulin expression in OPCs differentiated in the presence or absence of rapamycin. Immunodetection of Sirt2 and β-IV tubulin in OPCs after 3d differentiation *in vitro*. Expression of both Sirt2 (top panels) and β-IV tubulin (bottom panels) were reduced in differentiating OPCs in the presence of 15 nM rapamycin for 3 days. Rhodamine-conjugated secondary antibody was used for immunodetection of both proteins; nuclei were stained with DAPI.

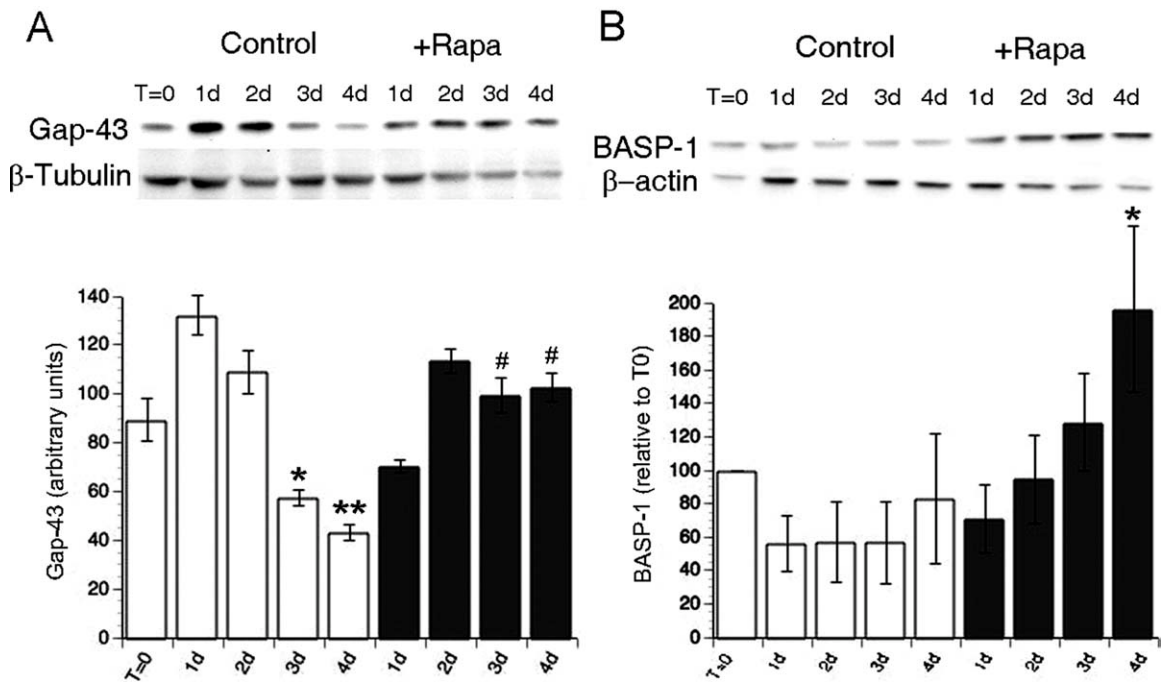

Fig. 7. Identification of Gap43/neuromodulin and BASP-1 as novel targets of the mTOR pathway inhibited during OPC differentiation. Western immunoblot analysis and quantification of Gap-43 (**A**) and BASP-1 (**B**) expression during a differentiation time course *in vitro*. Results confirm induction of Gap-43 and BASP-1 with mTOR inhibition. A: $^{*}P = 0.01$ versus 1d ctl; $P \leq 0.02$ versus 1d ctl; $^{\#}P < 0.005$ versus 3d or 4d ctl. B: $^{*}P = 0.01$ versus 4d ctl.

Regulators of OPC Differentiation, Fyn, QKI, and Gpr17, Are Part of the mTOR Proteome

We identified several proteins regulated by mTOR with known functions in coordinating oligodendrocyte differentiation (Table 2). These included two positive mediators of differentiation, the Src-like kinase, Fyn (Biffiger et al., 2000; Osterhout et al., 1999; Sperber et al., 2001), and the RNA-binding protein, quaking I (QKI) (Chen et al., 2007; Larocque et al., 2005; Zhao et al., 2006a), both are downregulated upon inhibiting mTOR signaling. Validation of these results by Western blot analysis revealed that Fyn expression increased in oligodendrocytes from 2 to 4 days of differentiation in control cultures, but was inhibited in the presence of rapamycin (Fig. 8A).

Similarly, the induction of two isoforms of QKI, QKI-6 and QKI-7, was inhibited in the presence of rapamycin by 4d of differentiation (Fig. 8B). In contrast, the QKI-5 isoform appeared unaffected by rapamycin (Fig. 8B). QKI exists as three isoforms in OPCs, QKI-5, 6, and 7 (Ebersole et al., 1996; Lu et al., 2003), which differ in their cellular localization and ability to promote oligodendrocyte differentiation (Chen et al., 2007; Wu et al., 1999; Zhao et al., 2006b). QKI-6 and 7 have potent effects to promote OPC maturation and myelination, whereas QKI-5 is thought to govern OPC proliferation and early differentiation but negatively affect myelination (Chen et al., 2007; Larocque et al., 2002, 2005).

In contrast to inhibiting positive mediators of oligodendrocyte differentiation, rapamycin elevated the expression of the G-protein-coupled receptor, Gpr17, a known inhibitor of oligodendrocyte differentiation (Chen et al., 2009) (Table 2). These results support the hypothesis that mTOR signaling regulates key mediators of differentiation that are upstream of the myelin synthesis program.

Comparison of the mTOR-Regulated Proteome With Gene Expression in Developing OPCs

The mTOR pathway is well known for its role in regulating the translation of specific classes of mRNAs, particularly through activation of the mTORC1 complex. However, mTOR signaling influences a variety of cellular processes including transcription directly or indirectly by virtue of its actions on multiple downstream targets (Cunningham et al., 2007). Moreover, analysis of our proteomic data suggested that many of the proteins identified are endpoints in the oligodendrocyte differentiation program rather than effectors that drive the decision to differentiate. This leads to the prediction that many of the proteomic changes we observed will be reflected by changes in mRNA expression during OPC differentiation. To determine how the differences we observed in the proteome by blocking mTOR-mediated differentiation align with changes in mRNA expression, we compared the proteins identified as altered by rapamycin treatment after 4d of differentiation with a previously reported microarray analysis of gene expression during OPC differentiation (Dugas et al., 2006). We compared the microarray data from OPC versus 3d differentiation to our protein data at 4d differentiation *in vitro* based on the rationale that changes in gene expression

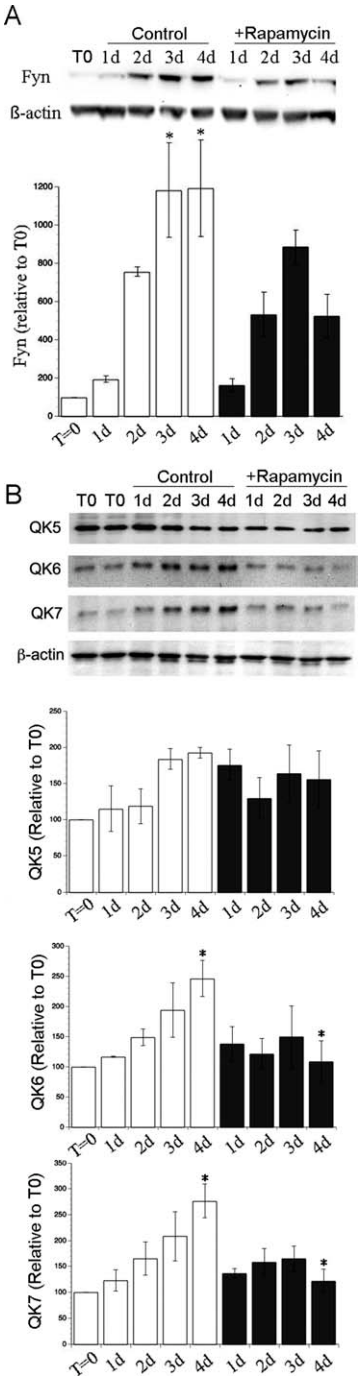

Fig. 8. Identification of Fyn, QKI-6, and QKI-7 as targets of the mTOR pathway during OPC differentiation. Western immunoblot analysis and quantification of Fyn (**A**) and QKI-5, 6, and 7 isoform (**B**) expression during a differentiation time course *in vitro*. A: Results show a decrease in Fyn, with rapamycin. $^*P < 0.01$ versus T_0; $P = 0.06$ 4d Rap versus 4d ctl. B: QKI-6 and 7, but not QKI-5 were inhibited in the presence of 10 nM rapamycin. $^*P < 0.01$ (4d ctl vs. T_0 and 4d rap vs. 4d ctl).

TABLE 3. Comparison of Protein and mRNA Expression in Oligodendrocytes at 3–4 Days of Differentiation

Identified proteins	Protein accession number	R/C (1–4)	Microarray (3 days)
Receptor expression-enhancing protein 5	IPI00360246	0.5	1.1
233 kDa protein	IPI00869671	0.6	1.1
2-Hydroxyacylsphingosine 1-β-galactosyltransferase	IPI00204426	0.6	1.0
26S protease regulatory subunit 7	IPI00421600	0.7	1.6
Glyceraldehyde-3-phosphate dehydrogenase	IPI00555252	0.7	1.5
Basic leucine zipper and W2 domain-containing protein 2	IPI00203352	0.7	1.5
Phosphoserine aminotransferase	IPI00331919	0.7	1.2
14-3-3 protein theta	IPI00196661	0.7	1.1
Putative uncharacterized protein Mrpl15	IPI00200739	0.7	1.1
Sorting nexin associated golgi protein 1	IPI00949260	0.7	1.1
Farnesyl pyrophosphate synthase	IPI00325147	0.7	1.1
Plectin 6	IPI00209000	0.7	1.0
Na-K-Cl cotransporter	IPI00212590	0.7	1.0
AP-2 complex subunit sigma	IPI00198371	0.7	1.0
ATP citrate lyase isoform 1	IPI00214665	0.7	1.0
Putative uncharacterized protein Map1a	IPI00198118	0.7	1.0
Acyl-CoA desaturase 2	IPI00464460	0.7	1.0
Heat shock protein HSP 90-β	IPI00471584	0.8	1.7
Interleukin-1 receptor accessory protein	IPI00211004	0.8	1.6
60S ribosomal protein L13a	IPI00655314	0.8	1.4
60S ribosomal protein L18a	IPI00192257	0.8	1.4
elongation factor Tu GTP-binding domain containing 2	IPI00370117	0.8	1.4
60S ribosomal protein L19	IPI00202214	0.8	1.3
ATP-binding cassette subfamily F member 1	IPI00421969	0.8	1.3
F-actin-capping protein subunit alpha-2	IPI00370681	0.8	1.3
Fructose-bisphosphate aldolase A	IPI00231734	0.8	1.3
ADP-ribosylation factor 3	IPI00231674	0.8	1.2
Elongation factor 2	IPI00203214	0.8	1.2
Proteasome (Prosome, macropain) 26S subunit, non-ATPase, 5 (predicted), isoform CRA_b	IPI00194471	0.8	1.1
Cytoplasmic dynein 1 light intermediate chain 2	IPI00207202	0.8	1.1
Staphylococcal nuclease domain-containing protein 1	IPI00471608	0.8	1.0
C-4 methylsterol oxidase	IPI00210465	0.8	1.0
Translationally controlled tumor protein	IPI00208306	0.8	1.0
Peroxiredoxin-1	IPI00211779	0.8	1.0
Microtubule-associated protein RP/EB family member 1	IPI00213299	0.8	1.0
Tubulin α-1A chain	IPI00189795	0.8	1.0
Coactosin-like protein	IPI00869481	0.8	1.0
Isoform 2 of α-adducin	IPI00231810	0.8	1.0
Guanine nucleotide-binding protein G(q) subunit alpha	IPI00230868	0.8	1.0
Lethal (2) giant larvae protein homolog 1	IPI00325878	0.8	1.0
EH domain-containing protein 1	IPI00360340	0.8	1.0
Catalase	IPI00231742	0.8	1.0
Myelin-oligodendrocyte glycoprotein	IPI00207944	0.8	1.0

would precede changes in protein expression. Overall, 711 of the 978 proteins from our proteomic analysis were listed in and compared to the microarray data tables. Interestingly, 71% of proteins we identified as reduced by inhibition of mTOR (and thus normally induced during differentiation) also had reduced mRNA expression (OPC/3d < 1). Similarly, 65% of the proteins upregulated by rapamycin had increased mRNA expression (OPC/3d > 1). Interestingly, we identified a subset of proteins (43) whose expression was reduced by inhibiting mTOR according to our proteomic analysis but was either unchanged or oppositely regulated at the level of mRNA expression during OPC differentiation (Table 3). These candidates represent proteins whose expression may be translationally regulated by mTOR.

Proteins Regulated by mTOR Signaling at 2d of Oligodendrocyte Differentiation

The high correlation of mTOR-regulated proteins with developmentally regulated gene expression in OPC differentiation supports the idea that mTOR regulates key proteins involved in the initial events of differentiation that are upstream of a large number of the changes we observed after 4 days of differentiation. Our previous studies demonstrated that the block of differentiation by mTOR inhibition occurred between 2 and 3 days at the transition from the late progenitor to the GalC+ immature oligodendrocyte (Tyler et al., 2009). Therefore, to identify early changes in the proteome by mTOR inhibition during OPC differentiation, we performed iTRAQ-MS analysis of protein samples isolated following 2d and 4d of differentiation plus or minus rapamycin. MS/MS spectra were obtained on two samples from each condition, because a maximum of eight total samples could be simultaneously analyzed in the iTRAQ analysis. The $O4^+/GalC^-$ late progenitor is the predominant cell type on day 2 *in vitro*, whereas $O4^+/GalC^+$ immature oligodendrocytes are generated by 4d of differentiation (Tyler et al., 2009).

We identified 653 proteins in the 2d/4d analysis (Supp. Info. Table 2). As expected, we observed the greatest change in mTOR-dependent protein expression between 2d and 4d of differentiation in control cells. However, we also identified several proteins whose

expression was regulated by mTOR signaling following 2d *in vitro*, before the transition to the immature oligodendrocyte stage. Specifically, 73 proteins (11%) were decreased (Rap/Ctrl $\leq$ 0.8) and another 70 proteins (11%) were increased (Rap/Ctrl $\geq$ 1.2) by mTOR inhibition following 2d of differentiation. To characterize these proteins further, we again performed functional analysis using the PANTHER classification system (Thomas et al., 2003), and the AmiGO search database. Similar to the 4d results, cytoskeletal proteins were identified as the largest class of proteins (13.3%) (Fig. 9A) downregulated by rapamycin treatment following 2d of differentiation. Other categories of downregulated proteins included: intermediate filament (6.7%), myelin protein (5%), and actin binding (3.3). Proteins that were upregulated in the presence of rapamycin included translation factor (6.7%) and translation initiation factor (6.7%), suggesting that the ability of mTOR signaling to finely tune the expression of specific transcripts via translational control plays a central role in regulating oligodendrocyte differentiation.

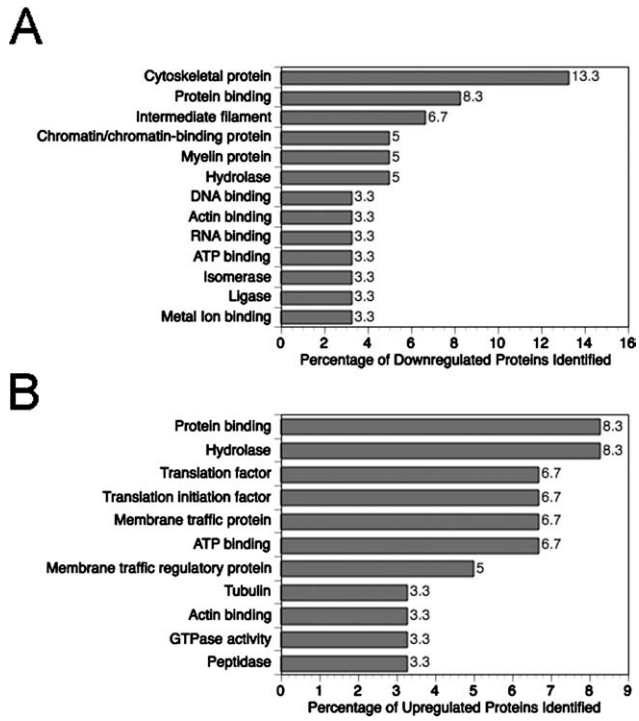

Fig. 9. Functional classification of changed proteins at 2d of oligodendrocyte differentation. **A, B:** Functional classification of the top classes of proteins downregulated (A) or upregulated (B) by rapamycin treatment during OPC differentiation.

To further the comparison of proteomic in this analysis and the transcriptome changes observed by Dugas et al. (2006), we compared changes in mRNA expression at 1 and 2 days of oligodendrocyte differentiation with changes in protein expression at 2d of differentiation. As for the 4d analysis, we identified a group of proteins (42%) that are potentially regulated at the level of translation, that is, downregulated in the presence of rapamycin and either unchanged or increased at the mRNA level at 1 and 2 days of differentiation (Table 4).

DISCUSSION

A number of extrinsic and intrinsic factors, including growth factors, their receptors, and specific transcription factors, have been identified that modulate oligodendrocyte

TABLE 4. Comparison of Protein and mRNA Expression in Oligodendrocytes at 1–2 d of Differentiation

Identified proteins	Protein accession number	R/C (2 day)	Microarray (1 day)
Talin	IPI00362014	0.5	1.0
Tryptophanyl-tRNA synthetase, cytoplasmic	IPI00780700	0.7	1.2
Isoform 1 of growth factor receptor-bound protein 2	IPI00203630	0.7	1.1
Isoform 1 of peroxisomal acyl-coenzyme A oxidase 1	IPI00211510	0.7	1.1
Catalase	IPI00231742	0.7	1.0
Structural maintenance of chromosomes protein 3	IPI00201289	0.7	1.2
Mitochondrial carrier homolog 2	IPI00764690	0.7	1.0
Ataxin-10	IPI00231553	0.8	1.1
Importin subunit β-1	IPI00204261	0.8	1.1
28 kDa heat- and acid-stable phosphoprotein	IPI00208277	0.8	1.1
Myb-binding protein 1A	IPI00205274	0.8	1.3
Protein disulfide-isomerase A4	IPI00212220	0.8	1.1
Hsd17b4 protein	IPI00326948	0.8	1.1
Stress-induced-phosphoprotein 1	IPI00213013	0.8	1.2
Lamin-B1	IPI00231418	0.8	1.0
Isoform 2 of reticulon-4	IPI00230986	0.8	1.0
Ring-box 1	IPI00366454	0.8	1.0
Actin-related protein 2	IPI00362072	0.8	1.0
Actin-related protein 2/3 complex subunit 2	IPI00764535	0.8	1.4
Translationally controlled tumor protein	IPI00208306	0.8	1.0
Heterogeneous nuclear ribonucleoprotein D-like	IPI00363719	0.8	1.1
Ribosome binding protein 1, partial	IPI00188079	0.8	1.1
ATP synthase subunit O, mitochondrial	IPI00195123	0.8	1.1
Isoform 1 of PC4 and SFRS1-interacting protein	IPI00213638	0.8	1.0
40S ribosomal protein SA	IPI00215107	0.8	1.1
Large neutral amino acids transporter small subunit 1	IPI00204778	0.8	1.1
Chaperonin subunit 6a	IPI00188111	0.8	1.2
Proteasome subunit beta type-1	IPI00191749	0.8	1.0
Glia maturation factor beta	IPI00230865	0.8	1.1
Leucine-rich PPR motif-containing protein, mitochondrial	IPI00360075	0.8	1.2
Isoform short of cytochrome b5	IPI00231013	0.8	1.0

differentiation. However, the intracellular signaling pathways that integrate and respond to the cues derived from these factors are not completely understood. Our previous study demonstrated that the mTOR signaling pathway is essential for the transition of OPCs from the late progenitor stage to a committed immature oligodendrocyte (Tyler et al., 2009). Using a proteomic approach, we now show several proteins with known involvement in oligodendrocyte differentiation are regulated as part of a differentiation program through mTOR signaling. Moreover, we have identified a large number of novel proteins regulated directly or indirectly by mTOR during oligodendrocyte differentiation.

The ability to quantitatively analyze up to eight distinct samples in the proteomic analyses provided the basis for these studies. Gel-free proteomics techniques developed over the years are now widely used for relative quantification of proteins in biological samples. Among these, iTRAQ has been very successful and allows up to eight samples to be compared quantitatively in a single experiment (Hu et al., 2006; Jain et al., 2008; Liu et al., 2007). Multiplexing provides better statistical power and thus identifies more reliable protein expression changes in a biological experiment. To focus on mTOR-dependent changes in protein expression, we performed iTRAQ-proteomics analysis on quadruplicate protein samples from control and rapamycin treated cultures on day 4 of differentiation. iTRAQ quantification accuracy relies profoundly upon iTRAQ reporter ion signal intensities and the precursor selection window of the mass spectrometer in addition to many other factors (sample preparation, chromatography, and isotopic purity of the iTRAQ reagents). By setting the highest possible TIS window on the 4800 TOF–TOF mass spectrometer, we were able to observe consistent changes for different peptides belonging to a given protein, resulting in reliable quantification of protein expression changes as reported in this study.

The mTOR-Regulated Proteome Defines an Oligodendrocyte Differentiation Program

The identification of an mTOR-regulated proteome, in combination with previously conducted microarray analysis of mRNA expression (Dugas et al., 2006), provides the basis to begin to formulate a hierarchy of the molecules that regulate the OPC differentiation program. Importantly, the mTOR-regulated proteome identified is a subset of the proteins identified in differentiating OPCs. As expected, a number of proteins identified are myelin proteins and other proteins necessary for myelin lipid synthesis such as enzymes involved in cholesterol and fatty acid biosynthesis. For example, oligodendrocyte-specific deletion of squalene synthase (fdft1), which we have now identified as a component of the mTOR proteome, demonstrated that cholesterol biosynthesis is an essential component for myelin production (Saher et al., 2005). However, many of these proteins are downstream in the differentiation process and likely are not critical for the initial commitment past the late progenitor stage. Therefore, it is probable that the expression levels of these proteins are indirectly regulated by mTOR as a consequence of mTOR signaling promoting the transition to the immature (GalC+) oligodendrocyte (Tyler et al., 2009).

Increased process extension and branching complexity are morphological features of cells that pass the transition from OPC to immature oligodendrocyte and initiate the program to become mature oligodendrocytes. Thus, it is not surprising that the largest group of proteins identified in our analyses as mTOR-induced were cytoskeletal proteins comprising multiple groups. However, our analysis also revealed alterations in proteins known to regulate the cytoskeletal changes associated with oligodendrocyte differentiation including the nonreceptor tyrosine kinase, Fyn, and the NAD-dependent histone deacetylase, Sirt2, both of which are known to directly regulate cytoskeletal changes during OPC differentiation. As such, they may provide a direct mechanism that defines mTOR-mediated changes in morphology during OPC differentiation. Fyn integrates signaling downstream of integrin receptors (Colognato et al., 2004; Laursen et al., 2009) and in turn modulates the activity of p190RhoGAP to downregulate RhoA activity and promote process extension (Liang et al., 2004; Wolf et al., 2001). Similarly, Sirt2 regulates the levels of α-tubulin acetylation during process extension (North et al., 2003; Tang and Chua, 2008). Sirt2 is a deacetylase for α-tubulin (North et al., 2003), but, paradoxically, its levels increase concurrently with increased α-tubulin acetylation during oligodendrocyte differentiation and process arborization (Li et al., 2007). Gain and loss of function studies support the hypothesis that Sirt2 acts as a counter-regulator to restrict the amount of acetylated tubulin and tightly regulate the cytoskeletal arborization during differentiation (Li et al., 2007).

A key finding of our previous study demonstrated that mTORC1 and mTORC2 each contribute to the regulation of oligodendrocyte differentiation through distinct mechanisms. Namely, mTORC2 modulates the mRNA levels of a subset of myelin genes, while mTORC1 regulates downstream targets via an alternative mechanism, which likely involves a direct effect on protein translation through the phosphorylation of p70S6K and 4EBP. However, it is of interest that the comparison of the proteome with the microarray data suggested that very few of the proteins identified as mTOR regulated are likely solely regulated by protein translation downstream of mTORC1. Future studies are required to determine whether targets identified in our proteomics screen are downstream of mTORC1 or mTORC2. However, our study identified QKI, an RNA-binding protein known to directly regulate posttranscriptional homeostasis of key transcripts required for OPC differentiation and myelination (Larocque et al., 2005; Li et al., 2000; Zhao et al., 2006a), as a target of the mTOR pathway. Accordingly, the relationship between mTOR signaling and QKI may provide a link between mTOR and protein translation during OPC differentiation. QKI exists in three isoforms in oligodendrocytes, and the exogenous expression of

any isoform promotes OPC differentiation *in vitro* (Chen et al., 2007). However, QKI-6 appears to be the most important isoform for oligodendrocyte differentiation and myelination *in vivo* (Zhao et al., 2006b). Conversely, QKI deficiency *in vivo* results in severe hypomyelination (Hardy et al., 1996). Interestingly, activity of QKI can be regulated by Fyn phosphorylation (Lu et al., 2005), suggesting that mTOR may influence the function of QKI via multiple mechanisms.

In addition to positively regulating oligodendrocyte differentiation, mTOR signaling appears to be important also for downregulating specific proteins that inhibit lineage progression such as GPR17, a G-protein-coupled receptor. GPR17 expression decreases in oligodendrocytes at the onset of myelination *in vivo*, and transgenic overexpression of GPR17 inhibits oligodendrocyte differentiation and myelination (Chen et al., 2009). Of particular interest is the observation that overexpression of GPR17 induces the expression of the inhibitor of DNA binding-2 (Id2) (Chen et al., 2009) whose expression alone is sufficient to arrest OPC differentiation at the late progenitor stage (Samanta and Kessler, 2004; Wang et al., 2001). These data suggest that increased expression of GPR17 in the presence of rapamycin may be responsible for the elevated levels of Id2 we observed in our previous study (Tyler et al., 2009).

Using an iTRAQ-based proteomic approach, we identified a number of significant mTOR-dependent changes in the expression levels of a diverse class of proteins. Although the possibility exists that mTOR regulates the stability of a subset of these proteins by direct phosphorylation, most of the targets identified are unlikely to be primary substrates of mTOR kinase activity. Instead, the functions of the mTOR kinase complexes during OPC differentiation likely involve direct phosphorylation events of well-characterized effectors of mTORC1 and mTORC2. For example, we previously demonstrated that p70S6K and 4EBP, downstream targets of mTORC1, are phosphorylated in the early stages of OPC differentiation *in vitro* (Tyler et al., 2009). In parallel, we showed that the phosphorylation of Akt (Ser473), a known target of mTORC2, is sustained during OPC differentiation and is rapamycin sensitive (Tyler et al., 2009). However, there are likely additional, noncanonical substrates of mTORC1 and mTORC2 that influence OPC differentiation. One intriguing possibility is that mTOR regulates the expression of a large number of proteins via the direct phosphorylation of one or a group of key transcription factors required for OPC differentiation. The overlap between the proteins we identified as targets of mTOR signaling by proteomic analysis and a previous genomic screen of changes in gene expression during oligodendrocyte differentiation supports this hypothesis (Dugas et al., 2006).

Finally, these studies provide the basis for analysis of the mTOR-regulated proteome *in vivo*. Defining which targets are downstream of the specific mTOR complexes will be important for defining linear and functional relationships of proteins regulating OPC differentiation and myelination. In addition, these classifications will be important in assessing how use of mTOR inhibitors systemically might affect either developmental myelination or remyelination processes in the CNS. There is considerable interest in using rapamycin analogs and in developing mTOR complex-specific inhibitors to treat cancer and for antiaging therapies. Shortly after the discovery of rictor/mTORC2, which was originally characterized as rapamycin-insensitive, Sabassov and colleagues (2006) reported that mTORC2 was inhibited by sustained treatment of cells with rapamycin. Similarly, we also found that sustained treatment of differentiating OPCs with rapamycin ($\geq$24 h) inhibited complex formation of mTORC2 as well as phosphorylation of Akt(473), a primary downstream target (Tyler et al., 2009), whereas shorter treatment times resulted in inhibition only of mTORC1 targets (Supp. Info. Fig. 1). Moreover, rapamycin inhibition of mTORC2 in OPCs is dose-dependent (Supp. Info. Fig. 1). It is clear that systemic rapamycin accesses the brain (Goebbels et al., 2010; Narayanan et al., 2009); however, whether the effective dose in the brain is adequate to inhibit mTORC2 as well as mTORC1 is unknown. Thus, the identification of mTOR complex-specific targets based on our proteomic analyses may prove highly beneficial for assessing consequences of systemic injections of mTOR complex inhibitors for the brain and for oligodendrocyte differentiation and myelination processes.

REFERENCES

Biffiger K, Bartsch S, Montag D, Aguzzi A, Schachner M, Bartsch U. 2000. Severe hypomyelination of the murine CNS in the absence of myelin-associated glycoprotein and fyn tyrosine kinase. J Neurosci 20:7430–7437.

Chen Y, Tian D, Ku L, Osterhout DJ, Feng Y. 2007. The selective RNA-binding protein quaking I (QKI) is necessary and sufficient for promoting oligodendroglia differentiation. J Biol Chem 282:23553–23560.

Chen Y, Wu H, Wang S, Koito H, Li J, Ye F, Hoang J, Escobar SS, Gow A, Arnett HA, et al. 2009. The oligodendrocyte-specific G protein-coupled receptor GPR17 is a cell-intrinsic timer of myelination. Nat Neurosci 12:1398–1406.

Colognato H, Ramachandrappa S, Olsen IM, ffrench-Constant C. 2004. Integrins direct Src family kinases to regulate distinct phases of oligodendrocyte development. J Cell Biol 167:365–375.

Cunningham JT, Rodgers JT, Arlow DH, Vazquez F, Mootha VK, Puigserver P. 2007. mTOR controls mitochondrial oxidative function through a YY1-PGC-1α transcriptional complex. Nature 450:736–740.

Dugas JC, Tai YC, Speed TP, Ngai J, Barres BA. 2006. Functional genomic analysis of oligodendrocyte differentiation. J Neurosci 26:10967–10983.

Ebersole TA, Chen Q, Justice MJ, Artzt K. 1996. The quaking gene product necessary in embryogenesis and myelination combines features of RNA binding and signal transduction proteins. Nat Genet 12:260–265.

Fox MA, Afshari FS, Alexander JK, Colello RJ, Fuss B. 2006. Growth conelike sensorimotor structures are characteristic features of post-migratory, premyelinating oligodendrocytes. Glia 53:563–566.

Goebbels S, Oltrogge JH, Kemper R, Heilmann I, Bormuth I, Wolfer S, Wichert SP, Mobius W, Liu X, Lappe-Siefke C, et al. 2010. Elevated phosphatidylinositol 3,4,5-trisphosphate in glia triggers cell-autonomous membrane wrapping and myelination. J Neurosci 30:8953–8964.

Hardy RJ, Loushin CL, Friedrich VL Jr, Chen Q, Ebersole TA, Lazzarini RA, Artzt K. 1996. Neural cell type-specific expression of QKI proteins is altered in quakingviable mutant mice. J Neurosci 16:7941–7949.

Harrington EP, Zhao C, Fancy SP, Kaing S, Franklin RJ, Rowitch DH. 2010. Oligodendrocyte PTEN is required for myelin and axonal integrity, not remyelination. Ann Neurol 68:703–716.

Hu J, Qian J, Borisov O, Pan S, Li Y, Liu T, Deng L, Wannemacher K, Kurnellas M, Patterson C, et al. 2006. Optimized proteomic analysis of a mouse model of cerebellar dysfunction using amine-specific isobaric tags. Proteomics 6:4321–4334.

Jain MR, Bian S, Liu T, Hu J, Elkabes S, Li H. 2009. Altered proteolytic events in experimental autoimmune encephalomyelitis discovered by iTRAQ shotgun proteomics analysis of spinal cord. Proteom Sci 7:25.

Jain MR, Liu T, Hu J, Darfler M, Fitzhugh V, Rinaggio J, Li H. 2008. Quantitative proteomic analysis of formalin fixed paraffin embedded oral HPV lesions from HIV patients. Open Proteom J 1:40–45.

Keller A, Nesvizhskii AI, Kolker E, Aebersold R. 2002. Empirical statistical model to estimate the accuracy of peptide identifications made by MS/MS and database search. Anal Chem 74:5383–5392.

Kim DH, Sarbassov DD, Ali SM, King JE, Latek RR, Erdjument-Bromage H, Tempst P, Sabatini DM. 2002. mTOR interacts with raptor to form a nutrient-sensitive complex that signals to the cell growth machinery. Cell 110:163–175.

Korshunova I, Caroni P, Kolkova K, Berezin V, Bock E, Walmod PS. 2008. Characterization of BASP1-mediated neurite outgrowth. J Neurosci Res 86:2201–2213.

Larocque D, Galarneau A, Liu HN, Scott M, Almazan G, Richard S. 2005. Protection of p27(Kip1) mRNA by quaking RNA binding proteins promotes oligodendrocyte differentiation. Nat Neurosci 8:27–33.

Larocque D, Pilotte J, Chen T, Cloutier F, Massie B, Pedraza L, Couture R, Lasko P, Almazan G, Richard S. 2002. Nuclear retention of MBP mRNAs in the quaking viable mice. Neuron 36:815–829.

Laursen LS, Chan CW, ffrench-Constant C. 2009. An integrin-contactin complex regulates CNS myelination by differential Fyn phosphorylation. J Neurosci 29:9174–9185.

Li W, Zhang B, Tang J, Cao Q, Wu Y, Wu C, Guo J, Ling EA, Liang F. 2007. Sirtuin 2, a mammalian homolog of yeast silent information regulator-2 longevity regulator, is an oligodendroglial protein that decelerates cell differentiation through deacetylating α-tubulin. J Neurosci 27:2606–2616.

Li Z, Zhang Y, Li D, Feng Y. 2000. Destabilization and mislocalization of myelin basic protein mRNAs in quaking dysmyelination lacking the QKI RNA-binding proteins. J Neurosci 20:4944–4953.

Liang X, Draghi NA, Resh MD. 2004. Signaling from integrins to Fyn to Rho family GTPases regulates morphologic differentiation of oligodendrocytes. J Neurosci 24:7140–7149.

Liu T, Donahue KC, Hu J, Kurnellas MP, Grant JE, Li H, Elkabes S. 2007. Identification of differentially expressed proteins in experimental autoimmune encephalomyelitis (EAE) by proteomic analysis of the spinal cord. J Proteom Res 6:2565–2575.

Lu Z, Ku L, Chen Y, Feng Y. 2005. Developmental abnormalities of myelin basic protein expression in fyn knock-out brain reveal a role of Fyn in posttranscriptional regulation. J Biol Chem 280:389–395.

Lu Z, Zhang Y, Ku L, Wang H, Ahmadian A, Feng Y. 2003. The quakingviable mutation affects qkI mRNA expression specifically in myelin-producing cells of the nervous system. Nucleic Acids Res 31:4616–4624.

McCarthy K, de Vellis J. 1980. Preparation of separate astroglial and oligodendroglial cell cultures from rat cerebral tissue. J Cell Biol 85:890–902.

Mosevitsky MI. 2005. Nerve ending "signal" proteins GAP-43, MARCKS, and BASP1. Int Rev Cytol 245:245–325.

Narayanan SP, Flores AI, Wang F, Macklin WB. 2009. Akt signals through the mammalian target of rapamycin pathway to regulate CNS myelination. J Neurosci 29:6860–6870.

Nesvizhskii AI, Keller A, Kolker E, Aebersold R. 2003. A statistical model for identifying proteins by tandem mass spectrometry. Anal Chem 75:4646–4658.

North BJ, Marshall BL, Borra MT, Denu JM, Verdin E. 2003. The human Sir2 ortholog, SIRT2, is an NAD+-dependent tubulin deacetylase. Mol Cell 11:437–444.

Osterhout DJ, Wolven A, Wolf RM, Resh MD, Chao MV. 1999. Morphological differentiation of oligodendrocytes requires activation of Fyn tyrosine kinase. J Cell Biol 145:1209–1218.

Saher G, Brugger B, Lappe-Siefke C, Mobius W, Tozawa R, Wehr MC, Wieland F, Ishibashi S, Nave KA. 2005. High cholesterol level is essential for myelin membrane growth. Nat Neurosci 8:468–475.

Samanta J, Kessler JA. 2004. Interactions between ID, OLIG proteins mediate the inhibitory effects of BMP4 on oligodendroglial differentiation. Development 131:4131–4142.

Sarbassov DD, Ali SM, Kim DH, Guertin DA, Latek RR, Erdjument-Bromage H, Tempst P, Sabatini DM. 2004. Rictor, a novel binding partner of mTOR, defines a rapamycin-insensitive and raptor-independent pathway that regulates the cytoskeleton. Curr Biol 14:1296–1302.

Sarbassov DD, Ali SM, Sabatini DM. 2005. Growing roles for the mTOR pathway. Curr Opin Cell Biol 17:596–603.

Sarbassov DD, Ali SM, Sengupta S, Sheen JH, Hsu PP, Bagley AF, Markhard AL, Sabatini DM. 2006. Prolonged rapamycin treatment inhibits mTORC2 assembly and Akt/PKB. Mol Cell 22:159–168.

Sperber BR, Boyle-Walsh EA, Engleka MJ, Gadue P, Peterson AC, Stein PL, Scherer SS, McMorris FA. 2001. A unique role for Fyn in CNS myelination. J Neurosci 21:2039–2047.

Tang BL, Chua CE. 2008. SIRT2, tubulin deacetylation, and oligodendroglia differentiation. Cell Motil Cytoskeleton 65:179–182.

Terada N, Kidd GJ, Kinter M, Bjartmar C, Moran-Jones K, Trapp BD. 2005. Beta IV tubulin is selectively expressed by oligodendrocytes in the central nervous system. Glia 50:212–222.

Thomas PD, Campbell MJ, Kejariwal A, Mi H, Karlak B, Daverman R, Diemer K, Muruganujan A, Narechania A. 2003. PANTHER: A library of protein families and subfamilies indexed by function. Genome Res 13:2129–2141.

Tyler WA, Gangoli N, Gokina P, Kim HA, Covey M, Levison SW, Wood TL. 2009. Activation of the mammalian target of rapamycin (mTOR) is essential for oligodendrocyte differentiation. J Neurosci 29:6367–6378.

Wang S, Sdrulla A, Johnson JE, Yokota Y, Barres BA. 2001. A role for the helix-loop-helix protein Id2 in the control of oligodendrocyte development. Neuron 29:603–614.

Werner HB, Kuhlmann K, Shen S, Uecker M, Schardt A, Dimova K, Orfaniotou F, Dhaunchak A, Brinkmann BG, Mobius W, et al. 2007. Proteolipid protein is required for transport of sirtuin 2 into CNS myelin. J Neurosci 27:7717–7730.

Wolf RM, Wilkes JJ, Chao MV, Resh MD. 2001. Tyrosine phosphorylation of p190 RhoGAP by Fyn regulates oligodendrocyte differentiation. J Neurobiol 49:62–78.

Wu J, Zhou L, Tonissen K, Tee R, Artzt K. 1999. The quaking I-5 protein (QKI-5) has a novel nuclear localization signal and shuttles between the nucleus and the cytoplasm. J Biol Chem 274:29202–29210.

Zhao L, Ku L, Chen Y, Xia M, LoPresti P, Feng Y. 2006a. QKI binds MAP1B mRNA and enhances MAP1B expression during oligodendrocyte development. Mol Biol Cell 17:4179–4186.

Zhao L, Tian D, Xia M, Macklin WB, Feng Y. 2006b. Rescuing qkV dysmyelination by a single isoform of the selective RNA-binding protein QKI. J Neurosci 26:11278–11286.

Zou J, Zhou L, Du XX, Ji Y, Xu J, Tian J, Jiang W, Zou Y, Yu S, Gan L, et al. 2011. Rheb1 is required for mTORC1 and myelination in postnatal brain development. Dev Cell 20:97–108.